NJC

New Journal of Chemistry

A journal for new directions in chemistry

Accepted Manuscript

This article can be cited before page numbers have been issued, to do this please use: L. Mandic, I. Dzeba, D. Jadresko, B. Mihaljevic, L. Biczok and N. Basari, *New J. Chem.*, 2020, DOI: 10.1039/D0NJ03465G.

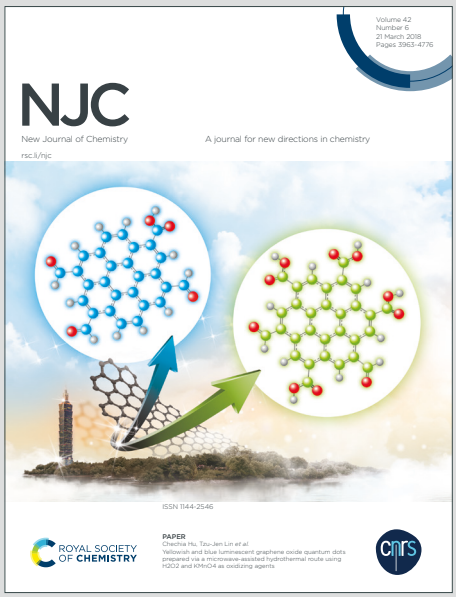

This is an Accepted Manuscript, which has been through the Royal Society of Chemistry peer review process and has been accepted for publication.

Accepted Manuscripts are published online shortly after acceptance, before technical editing, formatting and proof reading. Using this free service, authors can make their results available to the community, in citable form, before we publish the edited article. We will replace this Accepted Manuscript with the edited and formatted Advance Article as soon as it is available.

You can find more information about Accepted Manuscripts in the Information for Authors.

Please note that technical editing may introduce minor changes to the text and/or graphics, which may alter content. The journal's standard Terms & Conditions and the Ethical guidelines still apply. In no event shall the Royal Society of Chemistry be held responsible for any errors or omissions in this Accepted Manuscript or any consequences arising from the use of any information it contains.

View Article Online
DOI: 10.1039/D0NJ03465G

ARTICLE

Photophysical properties and electron transfer photochemical reactivity of substituted phthalimides

Received 00th January 20xx,
Accepted 00th January 20xx

DOI: 10.1039/x0xx00000x

Leo Mandić,[a,b] Iva Džeba,[b] Dijana Jadreško,[c] Branka Mihaljević,[b] László Biczók[d] and Nikola Basarić*[a]

Photochemical reactivity, photophysical and electrochemical properties for a series of *N*-adamantylphthalimides bearing carboxylic functional groups were investigated. Upon irradiations (with or without a triplet sensitizer), compounds undergo decarboxylation via a photoinduced electron transfer (PET) from the carboxylate to the phthalimide. UV-Vis and fluorescence pH titrations were used to determine pK_a values for the prototropic forms, which were put in connection with quantum yields of the reaction (Φ_R). Compounds bearing electron donors OH and OCH_3 at the phthalimide 4 position are fluorescent (Φ_F = 0.02-0.49) and PET takes place from both singlet and triplet excited states. Estimated rate constants for PET in the singlet excited states for methoxy- and amino-substituted phthalimides are (2.0 ± 0.1) × 10^9 $s^{-1}$and (3.4 ± 1.0) × 10^7 s^{-1}, respectively. Laser flash photolysis (LFP) was conducted to characterize triplet excited states, which are populated less efficiently for compounds with electron donors. The PET is reversible and the overall Φ_R depends on the rates for back electron transfer, protonation of the phthalimide radical anion and decarboxylation. Plausible photochemical and photophysical pathways depend on the phthalimide substituents, which is important for the use of phthalimide derivatives in organic synthesis and photocatalysis.

Introduction

Phthalimide is a chromophore whose photochemistry has been investigated for decades since the pioneering work of Kanaoka et al.[1] A rich array of phthalimide photoreactions, involving H-abstractions, cycloadditions and photoinduced electron transfer (PET),[2] found widespread applications in the synthesis of complex molecules and natural products.[3] For example, phthalimide derivatives in the triplet excited state undergo PET whereby phthalimide is an oxidant capable of reacting with donors having oxidation potential < 1.6 V vs. saturated calomel electrode.[4,5] These PET processes can initiate elimination of silyl groups,[6] or photodecarboxylation,[4,5] both of which were used in organic synthesis.[7] Thus, photodecarboxylation initiated macrocyclizations[8] and photocyclization of peptides,[9,10] photo-decaging,[11] enantioselective synthesis of benzodiazepines,[12] and cyclic aryl ethers,[13] as well as acetate,[14,15] benzyl,[16-18] or α-amino acid addition to phthalimides,[19] were documented. Furthermore, photodecarboxylations were also intensively investigated in the series of nonsteroidal anti-inflammatory drugs,[20-22] such as ketoprofen,[23-32] since the photodecarboxylation of these drugs leads to photoallergic responses.[33] Photoinduced decarboxylation is also important in the context of different photocatalytic processes.[34-41]

We have become interested in photodecarboxylation reactions initiated by phthalimide chromophore[42-44] and applied them in cyclizations with memory of chirality[45] and diastereoselective peptide cyclizations.[46] Furthermore, the photodecarboxylation efficiency was investigated in a series of phthalimide derivatives of adamantane amino acids, where we modified the distance between the electron donor (carboxylate) and the acceptor (phthalimide).[42] Thus, the decarboxylation efficiency was a useful handle to indirectly probe the rate of PET. Herein we describe the use of the same decarboxylation on adamantane derivative **1** (Scheme 1) as a probe for the PET reactivity in a series of substituted phthalimide derivatives **1**-**6**.

Phthalimide **1** was systematically modified by introducing electron-withdrawing and electron-donating substituents at the 4 position, which affected the photophysical properties of the molecules, as well as their photochemical reactivity. Although

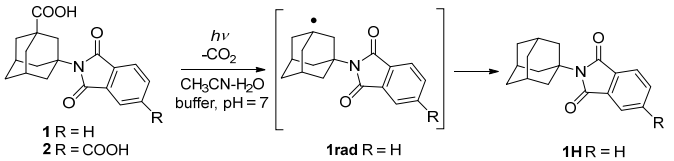

1 R = H
2 R = COOH
6 R = OCH_3
4 R = OH
5 R = NO_2
6 R = NH_2

Scheme 1. Photodecarboxylation of phthalimide derivatives.

[a] Department of Organic Chemistry and Biochemistry, Ruđer Bošković Institute, Bijenička cesta 54, 10000 Zagreb, Croatia, NB E-mail: nbasaric@irb.hr.
[b] Department of Material Chemistry, Ruđer Bošković Institute, Bijenička cesta 54, 10000 Zagreb, Croatia.
[c] Division for Marine and Environmental Research, Ruđer Bošković Institute, Bijenička cesta 54, 10000 Zagreb, Croatia.
[d] Institute of Materials and Environmental Chemistry, Research Centre for Natural Sciences, 1519 Budapest, P.O. Box 286, Hungary.

Electronic Supplementary Information (ESI) available: details on photochemical experiments, cyclic voltammetry, UV-vis and fluorescence spectroscopy, laser flash photolysis and MS and NMR spectra of pure compounds. See DOI: 10.1039/x0xx00000x

photochemical transformations of phthalimides are very useful in organic synthesis, not much is known about the photochemistry of their substituted derivatives,[47-49] with a notable exception of 4-aminophthalimide derivatives, which are known for their photochemical stability and high fluorescence quantum yields.[50-56] Photochemical reactivity and photophysical properties for **1**-**6** were investigated by preparative irradiations, steady-state and time-resolved fluorescence spectroscopy and laser flash photolysis (LFP). The photochemical experiments allowed for a complete elucidation of plausible pathways, particularly PET, which were put in connection with electrochemical properties of the molecules determined by cyclic voltammetry and pK_a values measured by UV-Vis and fluorescence pH titrations. Our main finding is that substituents on the phthalimide chromophore primarily affect the efficiency of intersystem crossing (ISC), where electron donors divert the photoreactions *via* singlet excited state instead of triplet. The detailed mechanistic study presented herein is important for the complete understanding of phthalimide photochemistry and rational planning of photoreactions for the use in organic synthesis.

Results and discussion

Synthesis and preparative photochemistry

Phthalimide derivatives **1**-**6** were prepared according to procedures published in literature precedent.[56,57] The synthesis involves condensation of 3-aminoadamantane-1-carboxylic acid with various 4-substituted phthalic anhydrides, and some subsequent transformations such as cleavage of the OMe ether by BBr_3, or reduction of the nitro group to amino.

Preparative irradiations of **1**-**6** were conducted in CH_3CN-H_2O, or acetone-H_2O mixtures (3:1 - v/v), in the presence of potassium carbonate to deprotonate the carboxylic functional group at the adamantane moiety. Namely, carboxylate is a better electron-donating group than the carboxylic acid (for example, 10-undecenoate in CH_3CN E_{ox} ≈ 1.38 V vs. Ag/AgCl, and 10-undecenoic acid in CH_3CN E_{ox} ≈ 1.85 V vs. Ag/AgCl).[58] A difference in the use of acetone or CH_3CN is anticipated since acetone acts as a triplet sensitizer with higher energy of the triplet excited state (E_T = 332 kJ mol^{-1})[59] than the one of *N*-alkylphthalimides (*N*-methylphthalimide E_T = 297 kJ mol^{-1})[59] where exergonic energy transfer to the phthalimide should be feasible.

The irradiations (300 nm) in acetone-H_2O mixture were generally selective, giving only decarboxylation products, **2H**-**4H**, analogous to the reaction shown in Scheme 1. On the other hand, irradiations in CH_3CN-H_2O gave, in addition to simple decarboxylation products, alcohols **3OH**-**5OH**, peroxides **4OOH**-**5OOH**, ketones **2COCH$_3$**-**4COCH$_3$** (Chart 1), and some unidentified products in the case of nitro derivative. All types of photoproducts were isolated and characterized by NMR and MS, and the yields of the isolated photoproducts are given in Table 1.

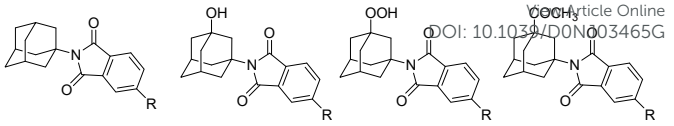

Chart 1. Products of photodecarboxylation in CH_3CN-H_2O.

Table 1. Irradiation conditions, conversions and product yields (%) for photolysis of phthalimides **1**-**6**.[a]

Compound solvent	Conversion[b] irradiation time	**1H**-**6H**	**3OH**-**5OH**	**4OOH**-**5OOH**	**2COCH$_3$**-**4COCH$_3$**
1	45 min	100			
CH_3CN-H_2O	100				
2	81	81	n.d.	n.d.	n.d.
acetone-H_2O	30 min				
2	66	43	n.d.	n.d.	23[c]
CH_3CN-H_2O	20 min				
3	88	88	n.d.	n.d.	n.d.
acetone-H_2O	30 min				
3	86	70	4	n.d.	12
CH_3CN-H_2O	30 min				
4	33	33	n.d.	n.d.	n.d.
acetone-H_2O	1 h				
4	70	42	16	8	4
CH_3CN-H_2O	4 h				
5	50	8	15	6	n.d.
CH_3CN-H_2O	20 min				
6	22	22	n.d.	n.d.	n.d.
CH_3CN-H_2O	4 h				

[a] Irradiations were conducted in acetone-H_2O or CH_3CN-H_2O (3:1 - v/v) using 10 lamps with the maximum output at 300 nm. The concentration of phthalimides was 1.5 mmol dm^{-3} (≈ 100 mg/200 mL), whereas K_2CO_3 concentration was 0.75 mmol dm^{-3}. The solutions were purged with Ar prior to irradiation. The yields correspond to isolated compounds, unless specified otherwise. [b] Conversion was calculated from ^{1}H NMR spectra of the crude irradiation mixture. [c] Yield obtained by HPLC analysis. n. d. = not detected.

Simple decarboxylation products are expected but the formation of alcohols, peroxides, and particularly ketones is surprising at first sight. Peroxide and alcohol photoproducts are probably formed by trapping of the radical (see Schemes 1 and 2) by traces of O_2 impurities in the solution. We have previously demonstrated that adamantyl radical formed in the decarboxylation reaction can be trapped by O_2 giving peroxides and alcohols.[42] Formation of ketones, on the other hand, suggests that an intermediate in the process is adamantyl carbanion that reacts with CH_3CN, although the reaction of adamantyl radical with CH_3CN to give ketones cannot be disregarded.

To elucidate the reaction mechanism for the formation of ketones, we performed irradiation of **3** in CH_3CN-H_2O and CH_3CN-D_2O. After the irradiation under identical conditions, the composition of the solution was analyzed by HPLC. Simple decarboxylation photoproducts **3H** and **3D** were isolated and

View Article Online
DOI: 10.1039/D0NJ03465G

ARTICLE

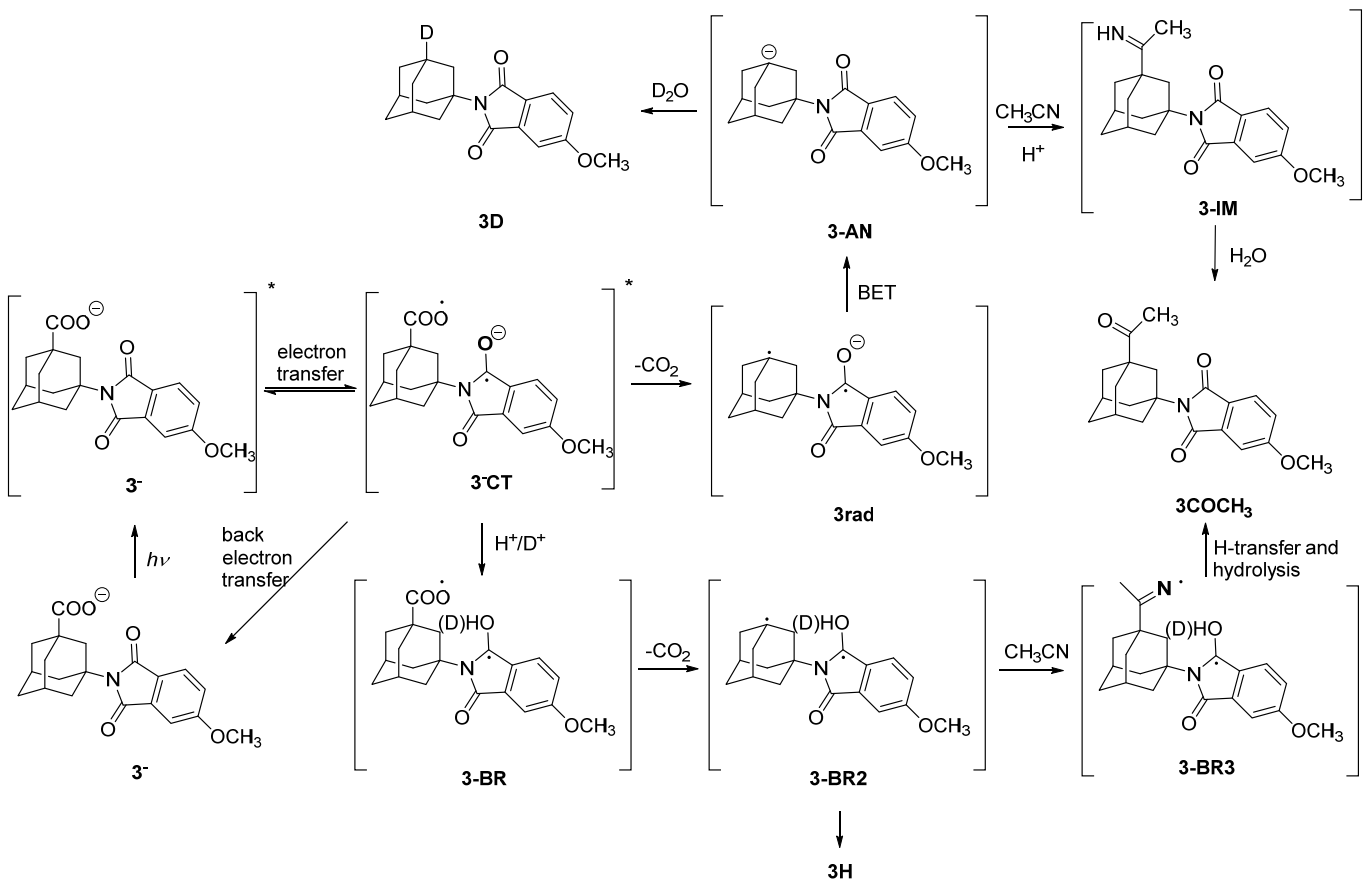

Scheme 2. Plausible mechanism for the formation of **3H**, **3D** and **3COCH$_3$**.

Table 2. Quantum efficiency for photoreaction (Φ_R) of **1**-**6**.[a]

Compound	CH_3CN-H_2O (1:1 - v/v)			acetone-H_2O (1:1 - v/v)		
	pH = 4.5	pH = 6.4	pH = 8.3	pH = 4.5	pH = 6.4	pH = 8.3
1	n. d.	n. d.	0.11[44]	n. d.	n. d.	0.5[44]
2	0.0083 ± 0.0006	n. d.	0.11 ± 0.01	0.079 ± 0.003	n. d.	0.34 ± 0.01
3	0.022 ± 0.002	n. d.	0.10 ± 0.01	n. d.	n. d.	0.35 ± 0.02
4	0.0018 ± 0.0001	0.011 ± 0.001	0.0052 ± 0.0005	0.00061 ± 0.00003	0.0032 ± 0.0002	0.0011 ± 0.0001
5	n. d.	n. d.	0.035 ± 0.002	n. d.	n. d.	0.10 ± 0.01
6	0.00045 ± 0.00003	n. d.	0.0046 ± 0.0001	0.0015 ± 0.0001	n. d.	0.0018 ± 0.0001

[a] Measured in CH_3CN-H_2O or acetone-H_2O (1:1 - v/v) in the presence of potassium phosphate buffer (c = 0.05 mol dm^{-3}). The samples were irradiated at 300 nm. The values correspond to the average of the results of three measurements. The photochemical transformation of **7** into **8** and **9** in acetone-H_2O (1:1 - v/v) or CH_3CN-H_2O (1:1- v/v) was used as a secondary actinometer (Φ_R = 0.30 ± 0.03).[42,60]

View Article Online
DOI: 10.1039/D0NJ03465G

ARTICLE

analyzed by NMR and MS to determine the extent of deuteration. Upon irradiation of **3** (10 min) in CH_3CN-H_2O the conversion to photoproducts was 80%, and the ratio of **3H**:**3COCH$_3$** was ≈ 9:1 (see the Experimental Section). On the other hand, under the same conditions in CH_3CN-D_2O, the conversion was 13% and the ratio of **3H(3D)**:**3COCH$_3$** was ≈ 4:1. In addition, deuterium incorporation took place, with 12% D incorporated according to MS. That is, 88% **3H** and 12% **3D** were formed. A significant decrease of the photoreaction conversion in D_2O was assigned to the equilibration of the excited state (**3**$^{-*}$) with the charge transfer state formed by PET, where the latter [**3**$^{-}$**CT**]* undergoes protonation vs. deuteration, decarboxylation or electron back transfer leading to the ground state **3**, or excited state **3**$^{-*}$. Thus, in the presence of D_2O, the slower D^+ addition to [**3**$^{-}$**CT**]* changes the plausible pathways and diminishes the importance of photoproduct formation compared to deactivation resulting in ground state **3**. Therefore, the deuterium effect provides a compelling evidence that efficiency of the sequence that involves PET and photodecarboxylation does not depend on the rate of PET only, but it depends also on the subsequent reactions, protonation and decarboxylation, that compete with the electron back transfer. This is a new mechanistic detail that in the previous reports has not been taken into account.[42,60]

Based on the deuterium incorporation in the molecule, plausible mechanism involves formation of carbanion **3-AN**, which is deuterated or reacts with the solvent (CH_3CN) to afford imine **3-IM**, which subsequently hydrolyses to **3COCH$_3$**. On the other hand, since the extent of deuteration did not exceed 12%, it is plausible that **3COCH$_3$** was formed in a parallel reaction of the adamantyl radicals **3-BR**, **3-BR2**, and **3BR-3**, which eventually react with CH_3CN to yield the **3COCH$_3$**. **3H** can also be formed from **3BR-2**. However, upon irradiation in CH_3CN-D_2O, incorporation of D is not expected since the only source of D is D_2O, and the homolytic cleavage of the H-OH (or D-OD) bond is energetically very demanding (the bond dissociation energy for H_2O is 460 kJ/mol). Note the different ratio of **3H**:**3COCH$_3$** which changes from 9:1 in CH_3CN-H_2O to 4:1 in CH_3CN-D_2O. It indicates the involvement of primary deuterium isotope effect with the value of ≈ 2.2, due to competition of deuteration with the attack of the solvent (CH_3CN) to the carbanion **3-AN**. The key reaction step in the carbanion reaction mechanism is back electron transfer (BET) from the phthalimide radical anion to the adamantyl radical (Scheme 2). To probe the feasibility of BET and to get general knowledge about redox properties of the molecules in PET, it is important to investigate their electrochemical properties (*vide infra*).

During the course of photolysis, the solution pH changes. Moreover, the investigated phthalimide derivatives can exist in different prototropic forms (*vide infra*), which should affect their reactivity. Therefore, the photoreactivity of phthalimide derivatives **2**, **4**, and **6** was investigated in solutions at different pH values (see Figs S1-S3 in the ESI). Compound **2**, which bears two carboxylic functional groups, undergoes more efficient photodecarboxylation in both solvents at pH > 6, whereas at pH > 7, the efficiency slightly decreases. The results indicate that the solution pH has to be basic enough to assure the deprotonation of the carboxylic functional group at the adamantane (electron donor), which facilitates the PET. However, formation of doubly charged anion by deprotonation of both carboxylic acids probably decreases the rate of PET. Furthermore, phthalimide **4** is a phenolic compound that can be deprotonated at high pH values, which significantly decreases the photodecarboxylation efficiency. Thus, **4** undergoes the most efficient photoreaction at pH 6-7, when the carboxylic group is deprotonated but the phenolic is not. On the other hand, phthalimide **6** is non-reactive (below pH 3) or very weakly reactive. Its reactivity increases very weakly in the pH region 3-7, in line with the anticipated pH region where the carboxylic functional group exhibits protonation equilibrium.

Quantum yields for the photochemical reactions (Φ_R) of **1**-**6** were measured in CH_3CN-H_2O and acetone-H_2O (1:1 - v/v) (Table 2). Instead of the base, solutions were buffered at pH values 4.5, 6.4 and 8.3 to have compounds present in different prototropic forms (*vide infra*). The samples were excited at 300 nm, and the photolysis of phthalimide **7** was used as a secondary actinometer (Φ_R = 0.3, Scheme 3).[60] A general trend appeared, that Φ_R is higher at pH values when the adamantane carboxylic acid is deprotonated, in agreement with the assumption that decarboxylation takes place after the initial PET from carboxylate to the excited phthalimide. Furthermore, for **1**-**3**, higher Φ_R was observed for the acetone triplet-sensitized reactions.

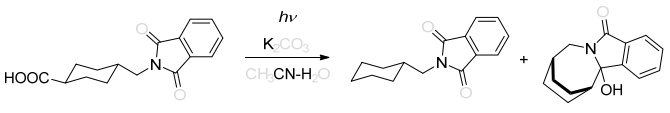

7 8 9

Scheme 3. Photoreaction of phthalimide **7** used as a secondary actinometer for the determination of reaction quantum yields.

Electrochemical properties

Cyclic voltammetry was conducted for **1**-**6** to determine their reduction potentials, which is important for the prediction of their PET reactivity. The measurements were performed in CH_3CN in the presence of NBu_4PF_6 as an electrolyte in the potential range from about 0.0 V to -2.0 V using Ag/AgCl (in 3 mol dm^{-3} NaCl) reference electrode. The measured reduction

View Article Online
DOI: 10.1039/D0NJ03465C

potentials expressed vs. ferrocene (Fc^0/Fc^+) are compiled in Table 3, whereas all details can be found in the ESI (Figs S4-S9). From the reduction potentials and estimated energies of the singlet excited states ($\Delta E_{0,0}$), obtained from the onsets of the absorption spectra, Gibbs free energies for PET ($\Delta_{ET}G°$) were calculated. Previous studies demonstrated that the energy of S_1 state, which corresponds to the location of the intersection of the normalized absorption and fluorescence spectra, barely differs from the energy of the onset of the absorption.[61,62] Therefore, the use of the latter quantity is a good approximation (see Figs S13 and S14 in the ESI). The obtained values suggest that PET from the S_1 state of all phthalimides should be thermodynamically feasible except for amino derivative **6**.

Table 3. Reduction potentials for 1-6,a energies for the excitation to S1 and calculated Gibbs free energy for PET in S1.

Compound	E_{red} / V vs. Fc^0/Fc^+	E_{S1} / kJ mol^{-1} [b]	$\Delta_{ET}G°$ / kJ mol^{-1} [c]
1	-1.98	356 (336 nm)	-69
2	-1.62 [d]	345 (347 nm)	-92
3	-2.05	310 (386 nm)	-16
4	-1.90 [d]	308 (389 nm)	-28
5	-1.21 -1.70 [e]	299 (400 nm)	-86
6	-2.17	260 (460 nm)	45

[a] The measurements were conducted in CH_3CN in the presence of 0.1 mol dm^{-3} NBu_4PF_6 as electrolyte. The reported value is the mean between the reduction and oxidation peak, unless stated otherwise. [b] The energy for the vertical excitation to S_1 (E_{S1}), estimated from the onset of the absorption spectrum, the wavelength is given in brackets. [c] Gibbs free energy for PET ($\Delta_{ET}G°$) was calculated according to: $\Delta_{ET}G^o = N_A e[E^o(D^{+\cdot}/D) - E^o(A/A^{-\cdot})] + w(D^{+\cdot}A^{-\cdot}) - \Delta E_{0,0}$, where e is the elementary charge, e = 1.602 × 10^{-19} C, N_A is the Avogadro constant, N_A = 6.022 × 10^{23} mol^{-1}, $E^o(D^{+\cdot}/D)$/V is the standard electrode potential of the donor radical cation formed in PET (0.96 V vs. Fc^0/Fc^+ value taken from the ref. [58]), and $E^o(A/A^{-\cdot})$/V is the standard electrode potential of the acceptor radical anion (the same as the measured E_{red}), $w(D^{+\cdot}A^{-\cdot})$ is the electrostatic work that accounts for the effect of Coulombic attraction in the photoproducts (the estimated value is 3.4 kJ mol^{-1}, see the SI), $\Delta E_{0,0}$ is the vibrational zero electronic energy of the excited donor, approximated as E_{S1}.[63] [d] Irreversible reduction peak. [e] Two reduction processes, both reversible.

Photophysical properties

Absorption spectra for phthalimides **1**-**6** were measured in CH_3CN (Figs S10-S15 in the ESI). Phthalimides **1** and **2** exhibit the typical absorption spectra of *N*-alkylphthalimides with a low-energy maximum at ≈ 300 nm, whereas strong electron-donating and -withdrawing groups significantly affect the spectra. Thus, absorption spectra of **3** and **4**, compounds that bear moderately electron-donating groups, exhibit additional low energy band stretching between 320 and 380 nm. The effect is more pronounced with amino substitution, so that absorption of **6** is characterized by a low-energy maximum at ≈ 370 nm. Note that this band is solvatochromic, due to a CT character of the aminophthalimide chromophore.[50-56] On the other hand, electron-withdrawing nitro group also affects the spectrum by introducing a lower energy absorption band at 350-400 nm with low absorptivity.

In the series of investigated phthalimides **1**-**6**, only derivatives **3**, **4** and **6** exhibit a significant fluorescence, whereas for the other molecules, fluorescence quantum yield (Φ_F) was lower

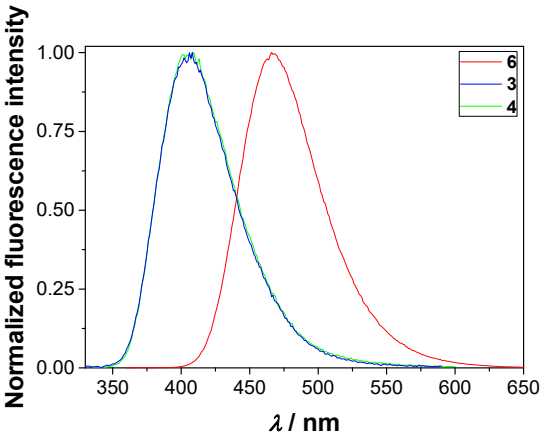

Figure 1. Normalized emission spectra of **3** (λ_{exc} = 310 nm), **4** (λ_{exc} = 310 nm) and **6** (λ_{exc} = 350 nm) in CH_3CN at 25 °C.

than 10^{-4}. In addition, fluorescence was measured for **3H**, **4H** and **6H** (See Fig S16). The fluorescence spectra (Fig 1) and Φ_F were determined in aprotic solvent (CH_3CN) and in aqueous solvent at two pH values (4.5 and 8.3), where the adamantane carboxylic acid should be protonated or not (Table 4). Under the same conditions, time-correlated single-photon counting measurements (TC-SPC) were performed to reveal singlet excited state lifetimes (τ_F) and potentially elucidate processes that lead to the deactivation from the singlet excited state.

The most intensively fluorescent compound is **6**, whose spectral and photophysical properties in CH_3CN are analogous to those reported for **6H**.[56] Decay of fluorescence in CH_3CN was fit to an exponential function revealing similar τ_F for both compounds. However, a small difference in Φ_F at pH 4.5 and 8.3 was observed for **6** in CH_3CN-H_2O 1:1 v/v mixture, which was attributed to the protonation equilibrium of the carboxylic acid. At higher pH, a good electron donor carboxylate is formed but PET to the phthalimide moiety is inefficient in the S_1 excited state due to a positive $\Delta_{ET}G°$ of the process. The τ_F values for **6** in CH_3CN-H_2O 1:1 v/v mixture diminished from 7.30 to 5.84 ns when the pH was raised from 4.5 to 8.3, in line with the lowering of the Φ_F. Assuming that the τ_F decrease arises from PET (possible only when the acid is deprotonated), k_{et} = (3.4 ± 1.0) × 10^7 s^{-1} was estimated for the rate constant of this process at pH 8.3. At the low wavelength region of the fluorescence spectrum (460 nm), a short-lived emission of ≈ 0.4 ns lifetime also appeared indicating the partial protonation of the amine moiety in the S_1 excited state.

Methoxy-substituted compound **3** has a modest Φ_F in CH_3CN, presumably due to competing intersystem crossing ISC (*vide infra*). The decay of fluorescence was fit to a sum of two exponentials (Table 4), with increasing contribution of a long-lived component at higher wavelengths (Table S1). The dual-exponential fluorescence decay kinetics is probably attributed to the two torsional isomers differing in the orientation of the methoxy substituent relative to the phthalimide group.

View Article Online
DOI: 10.1039/D0NJ03465G

ARTICLE

Table 4. Fluorescence quantum yields (Φ_F)[a] and fluorescence decay times (τ_F)[b]

Compound	In CH_3CN		in CH_3CN-H_2O (1:1 - v/v)			
			pH = 4.5		pH = 8.3	
	Φ_F	τ_F / ns	Φ_F	τ_F / ns	Φ_F	τ_F / ns
3	0.024 ± 0.002	1.68 ± 0.01 16.0 ± 0.4	0.49 ± 0.05	4.6 ± 0.2 24.7 ± 1.0	0.017 ± 0.006	0.46 ± 0.01 23.7 ± 1.0
3H	0.008 ± 0.001	n.d.	0.30 ± 0.03	n.d.	n. d.	n.d.
4	0.037 ± 0.003	2.33 ± 0.08 14.7 ± 0.3	0.013 ± 0.001	≤ 0.1 2.4 ± 0.3 22.0 ± 0.8 [c]	0.018 ± 0.001	1.88 ± 0.01
4H	0.027 ± 0.006	n.d.	0.019 ± 0.001	n.d.	n. d.	n.d.
6	0.66 ± 0.03	17.2 ± 0.2	0.11 ± 0.01	0.4 ± 0.1 7.32 ± 0.05	0.087 ± 0.002	0.4 ± 0.1 5.84 ± 0.07
6H	0.60 ± 0.06	18.98 ± 0.02 [56]	0.12 ± 0.01	n.d.	n. d.	n.d.

[a] Measured using quinine sulfate in 0.5 mol dm^{-3} H_2SO_4 (Φ_F = 0.55) or 9-cyanoanthracene in cyclohexane (Φ_F = 0.92) as a reference.[59] The data represent the average of the results obtained at three excitation wavelengths. The error corresponds to maximum absolute deviation. [b] Singlet excited state lifetimes were measured by time-correlated single photon counting (TC-SPC). At least three decays were collected at three wavelengths and the average value is reported, and the error corresponds to maximum absolute deviation Pre-exponential factors depend on the detection wavelength and they are reported in Table S1 in the ESI. [c] The pre-exponential factor of this component has ≤ 0.7 % contribution to the sum of all pre-exponential factors.

Similar behavior has been reported for 2-methoxyanthracene,[64] and 6-methoxy-1-methylquinolinium.[65] In aqueous solvent, at pH 4.5 the Φ_F of **3** is about 20 times higher than in CH_3CN, whereas both decay components exhibit significantly longer lifetime. Red-shifts in the absorption and fluorescence spectra were also observed, implying that the energy of the S_1 state diminishes when CH_3CN solvent is replaced by CH_3CN-H_2O 1:1 v/v mixture. This effect probably reduces the rate of triplet formation leading to higher Φ_F and longer τ_F. The alteration of pH from 4.5 to 8.3 results in considerable decrease in the dominant fluorescence lifetime component of **3**, probably due to PET from the deprotonated carboxylate to methoxyphthalimide in the S_1 excited state. From the difference in lifetimes, k_{et} = (2.0 ± 0.1) × 10^9 s^{-1} was derived for the rate constant of PET. The two order of magnitude higher k_{et} for **3** than for **6** is in accordance with the smaller estimated $\Delta_{ET}G°$ for the former compound (Table 3).

In CH_3CN, the OH-substituted phthalimide **4** has similar photophysical properties as the methoxy compound **3**, with a modest Φ_F and dual-exponential fluorescence decay. In contrast, the addition of water leads to substantial Φ_F decrease in CH_3CN-H_2O mixture at pH 4.5 because proton transfer from the OH group to water becomes an efficient deactivation pathway of the S_1 excited state. The short-lived fluorescence component, whose lifetime is less than the time-resolution of our instrument (≤ 0.1 ns), indicates that the excited state proton transfer (ESPT) is very fast. This decay component weakens as the monitoring wavelengths is raised, and the amplitude of a longer-lived emission (τ_F = 2.4 ns) gradually grows. The latter fluorescence is attributed to the phenolate form, whose fluorescence emerges at longer wavelengths. Similar behavior was found at pH 6.4 where the COOH moiety of **4** is deprotonated but the OH substituent remains unchanged (Table S1). At pH 8.3, the phenolate form of **4** is produced in the ground state. Hence, exponential fluorescence decay was observed with 1.88 ns lifetime at all wavelengths.

Acid-base properties of substituted phthalimides

Fluorescence measurements and the dependence of photodecarboxylation efficiencies on pH suggested that phthalimide derivatives exhibit different photophysical properties and react differently depending on their prototropic forms. Therefore, we investigated acid-base properties of molecules by UV-Vis and fluorescence pH titrations.

Fluorescence titration for **3** was conducted in the pH region 3.5-7.5, where a significant fluorescence quenching was observed (Fig 2) with no change in the absorption spectra. The finding was rationalized by quenching of fluorescence via electron transfer in the S_1 excited state from carboxylate, which is formed upon deprotonation with increasing solution basicity (Eq 1), to the methoxy-substituted phthalimide moiety. The fluorescence titration data was processed by nonlinear regression analysis using the Specfit software, allowing for the estimation of the pK_a value for deprotonation of the adamantyl carboxylic functional

Table 5. pK_a values for phthalimide derivatives determined by UV-Vis or fluorescence pH titration.[a]

Compound / equilibrium	Spectroscopic method	pK_a
3 / RCOOH→RCOO$^-$ + H$^+$	Fluorescence	5.56 ± 0.01
4 / ROH→RO$^-$ + H$^+$	UV-Vis	7.36 ± 0.01
	Fluorescence	7.32 ± 0.01
4H / ROH→RO$^-$ + H$^+$	UV-Vis	7.36 ± 0.02
	Fluorescence	7.28 ± 0.02
6 / RCOOH→RCOO$^-$ + H$^+$	Fluorescence	6.0 ± 0.2
RNH_3^+→RNH_2 + H$^+$	UV-Vis	1.65 ± 0.02
RNH_3^+→RNH_2 + H$^+$	Fluorescence	2.11 ± 0.03
6H / RNH_3^+→RNH_2 + H$^+$	UV-Vis	2.02 ± 0.04
RNH_3^+→RNH_2 + H$^+$	Fluorescence	2.30 ± 0.04

[a] The titrations were conducted in CH_3CN-H_2O in the presence of KCl (c = 2 mol dm^{-3}) (for **6** and **6H**) or phosphate buffer (c = 0.05 mol dm^{-3}) (for **3**, **4**, and **4H**) at 25 °C.

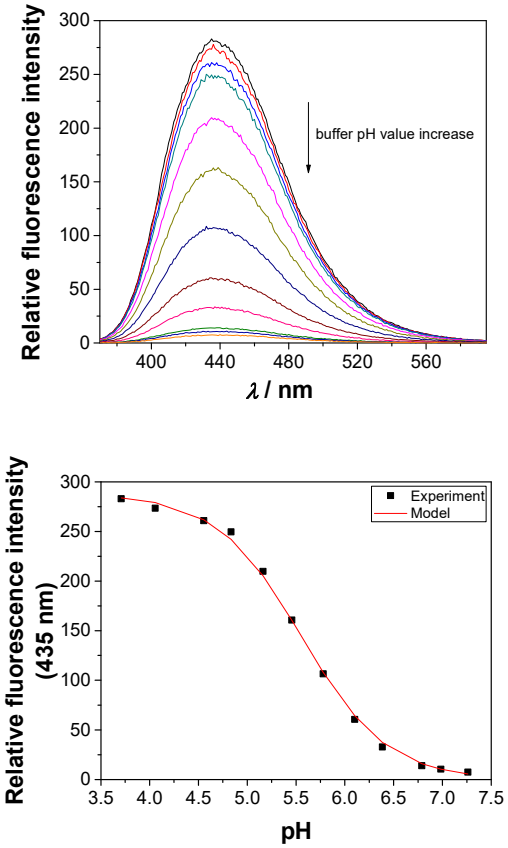

Figure 2. Emission spectra of **3** (λ_{exc} = 350 nm, c = 9.13 × 10^{-6} mol dm^{-3}) in CH_3CN-H_2O (1:1 -v/v) in the presence of phosphate buffer (c = 0.05 mol dm^{-3}) at different buffer pH values (top) and dependence of the fluorescence intensity at 435 nm on pH (bottom); black dots are the measured values and the red line corresponds to the calculated values obtained by nonlinear regression analysis with the Specfit software. The measurements were conducted at 25 °C.

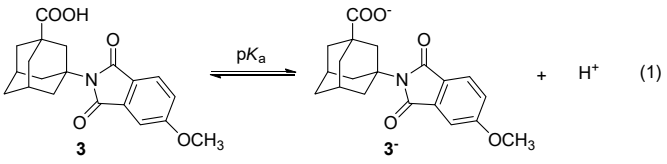

group (Table 5). Furthermore, it is reasonable to assume that all compounds **1**-**6** probably have similar values for the pK_a of the adamantane carboxylic group since the changes at the distant phthalimide site should not affect its acidity.

For compound **4** at low pHs, the fluorescence is very weak in the 400-500 nm range, where its emission is expected, due to the very rapid ESPT bringing about singlet excited phenolate form. The increase of the solution basicity enhances the phenolate fluorescence appearing at longer wavelengths as a result of concomitant **4** deprotonation in the ground and singlet excited states (Fig 3). The alteration of the UV-Vis spectra (Fig S17) implies the formation of the phenolate absorbing at higher wavelengths in line with the equilibrium for the phenol deprotonation in the ground state. Processing of the fluorescence and UV-Vis data by nonlinear regression analysis provided similar pK_a values for the deprotonation of **4** in the ground state, which are somewhat lower than for the parent phenol **4H** (Table 5, Figs S18 and S19) because the electron-withdrawing effect of the imide stabilizes the double negative charge formed under basic conditions (Eq 2).

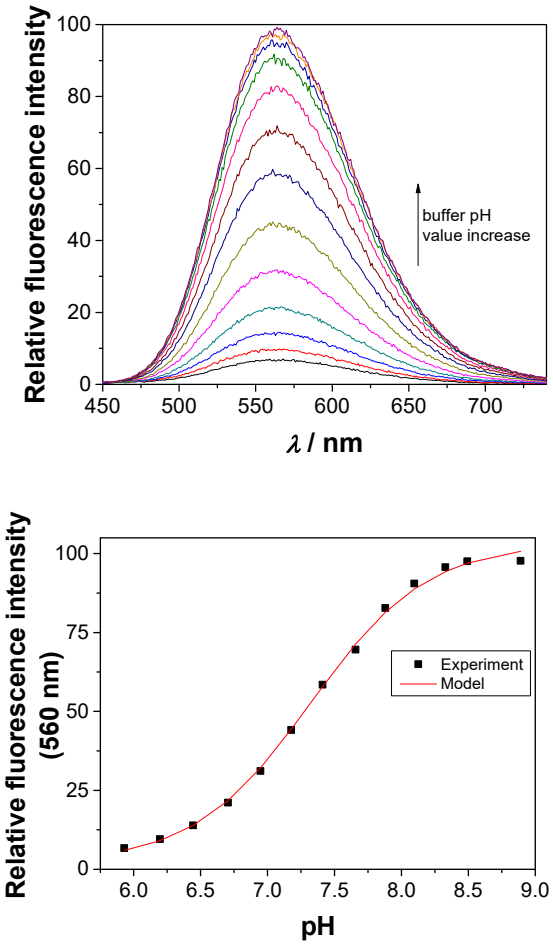

Figure 3. Emission spectra of **4** (λ_{exc} = 380 nm, c = 2.72 × 10^{-5} mol dm^{-3}) in CH_3CN-H_2O (1:1 - v/v) in the presence of phosphate buffer (c = 0.05 mol dm^{-3}) at different buffer pH values (top) and dependence of the fluorescence intensity at 560 nm on pH (bottom); black dots are the measured values and the red line corresponds to the calculated values derived by nonlinear regression analysis with the Specfit software. The measurements were conducted at 25 °C.

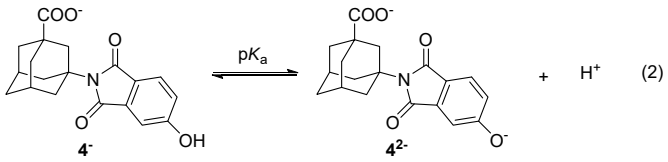

Protonation of the NH_2 group of **6** significantly quenches fluorescence (Fig S20 in the ESI) and induces pronounced changes in the absorption spectra (Fig 4). Processing of the UV-Vis and fluorescence titration data for **6** and **6H** measured in the acidic region allowed for the estimation of the amine pK_a. The estimated values from the UV-Vis and fluorescence data are somewhat different (Table 5), and imperfect fit was obtained from the fluorescence titration. The discrepancy may be due to the different pK_a values of the ground and excited singlet states. It is known that ammonium ions become more acidic in the excited S_1 state.[66-68] The same trend in the UV-Vis and fluorescence spectra was observed for **6H** for which similar pK_a values were revealed from the titrations. The increase of the solution pH above 4.5, very weakly quenched fluorescence for **6**, but no change was found for **6H**, confirming that the quenching originates from the deprotonation of the carboxylic group (Eq 3), which was also indicated by TC-SPC (*vide supra*).

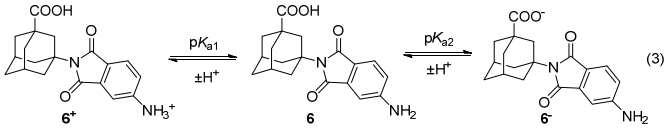

Laser flash photolysis (LFP) and properties of triplet excited states

Phthalimides substituted with electron-donating substituents participate in PET reactions from S_1 state, as indicated by fluorescence measurements. However, triplet excited state reactions for imides are more ubiquitous.[1,2] Furthermore, regardless of the phthalimide substitution, acetone sensitization should give rise to phthalimide triplet excited states that undergo decarboxylation. To investigate triplet excited state properties of **1**-**6**, LFP measurements were conducted. Similar to the fluorescence measurements, LFP was conducted for CH_3CN and CH_3CN-H_2O solutions. The samples were excited at 266 nm, and the solutions were purged with N_2 or O_2, where a difference was anticipated since O_2 quenches triplet excited states, radicals and radical anions. For all data see Figs S24-S41 in the ESI.

Transient absorption spectra measured in CH_3CN are shown in Fig 5. For **2**-**4**, triplet excited states were detected, which exhibited 30-50 nm batochromically shifted maxima compared to unsubstituted **1** and the typical *N*-alkylphthalimides (λ_{max} = 330 nm).[42,69] The assignment to triplet excited states was based on the quenching with O_2 (Table 6). The efficiency for the formation of triplet states was estimated by comparing the intensity of transients immediately after the laser pulse with the one of *N*-methylphthalimide (Φ_{ISC} = 0.8)[70] for the optically matched solution at the excitation wavelength. However, due to batochromically shifted maxima for **2**-**4**, it is only a coarse approximation. Triplet excited state for **3** and **4** are formed about 50% less efficiently than for **1**, whereas for **2** the intersystem crossing (ISC) is almost three times less efficient than for **1**. Furthermore, the triplet excited state lifetime (τ) for **2** and **4** is about 30 times shorter than for methoxy-substituted phthalimide **3**. Although the reason for the shorter lifetime of triplet excited state of **2** (compared to **1**) is not clear, the difference between the τ of **3** and **4** may be due to photoinduced intermolecular H-atom transfer from phenolic group to carbonyl, an ubiquitous quenching mechanism for triplet excited carbonyl compounds.[71] Transient absorption data for nitro compound **5**, reveals a completely different behavior. Only a very short-lived transient was detected, absorbing at ≈ 330 and 350-450 nm, most probably corresponding to the triplet excited state of **5**, in line with the spectra of the triplet excited states of nitrobenzene derivatives. Thus, the nitro group significantly changed the photophysical properties of the molecule. On the other hand, the amino group

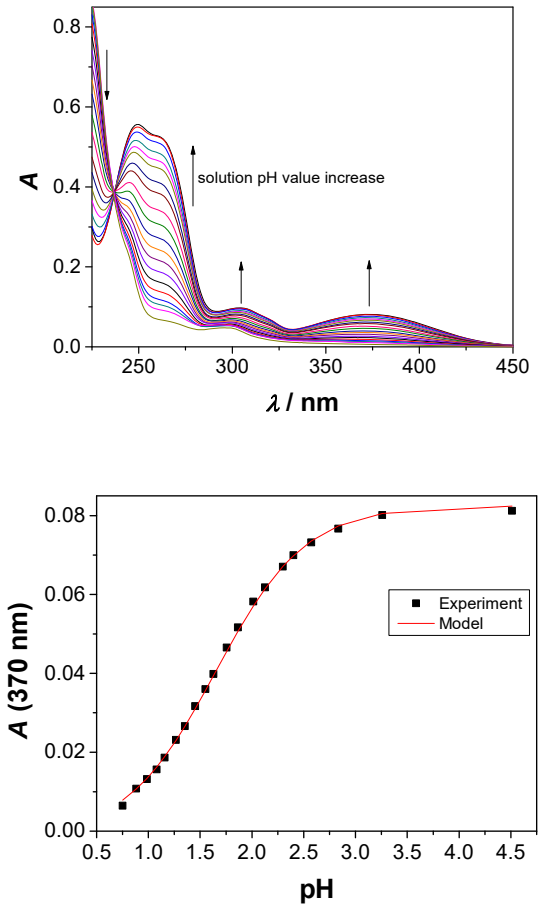

Figure 4. Absorption spectra of **6** (c = 1.75 × 10^{-5} mol dm^{-3}) in CH_3CN-H_2O (1:9 - v/v) in the presence of KCl (c = 2 mol dm^{-3}) at different pH values (left) and dependence of absorbance at 370 nm on pH (right); black dots are the measured values and the red line corresponds to the data calculated by nonlinear regression analysis with Specfit software. The measurements were conducted at 25 °C.

View Article Online
DOI: 10.1039/D0NJ04465C

in **6** gave rise to the formation of S_1 CT state, as revealed from the fluorescence measurement, that very inefficiently undergoes ISC. Nevertheless, the triplet state of **6** was detected (broad band 400-600 nm), assigned based on literature precedent,[72] albeit its signal was weak due to inefficient formation.

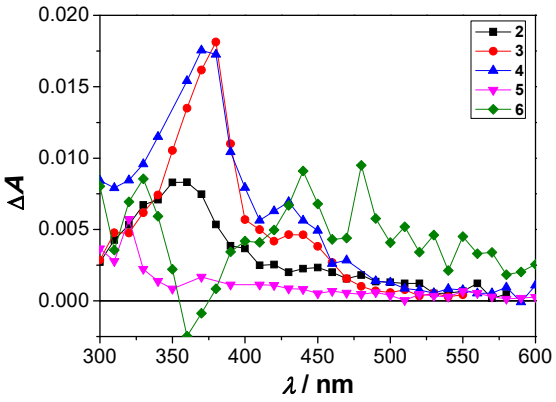

Figure 5. Transient absorption spectra of **2**-**6** in N_2-purged CH_3CN, recorded immediately after the laser pulse, within 10 ns (λ = 266 nm).

To probe for the PET from the triplet excited state, LFP measurements were conducted for **1**-**4**, at pH 4 and 7, where the adamantane carboxylic acid is protonated or not. We anticipated that the formation of the carboxylate would quench the triplet excited state of the phthalimide group, and result in the formation of phthalimide radical anion. For **1** we detected weak transients, which did not provide spectra with a clear pattern for two anticipated species. However, the decay of the triplet at pH 7 was faster compared to the one detected at pH 4. An additional long-lived transient was detected (τ = 150 µs) and tentatively assigned to the radical anion or ketyl radical based on comparison with the literature precedent.[44,68] From the two different rate constants for the decay of the phthalimide triplet at pH 7 and 4 (See Fig S25 and S26), the quenching rate constant can be calculated $k_q = (2.5 \pm 0.5) \times 10^6$ s^{-1}, which is too small for PET.

Phthalimides are known to undergo H-abstraction reactions giving rise to ketyl-like radicals.[1] To rule out that the detected transients in the photochemistry of **1** correspond to a ketyl radical, which undergoes deprotonation equilibrium, and thus, exhibit different lifetime depending on pH, we conducted measurements for *N*-methylphthalimide in CH_3CN-H_2O without buffer and in the presence of phosphate buffer at pH 4 and 7 (See Figs S42-S44). The transient absorption spectra at two pH values look the same with the maximum at 330 nm. The decay of the transient was fit to a sum of two exponentials with $\tau \approx 10$ µs and $\tau \approx 50$ µs, giving similar values for the decay times regardless of conditions. The short decay time (10 µs) was assigned to the triplet excited state of the phthalimide, whereas the long one (50 µs) probably corresponds to the ketyl radical that is not acidic enough to be deprotonated at pH 7, and therefore, does not exhibit pH-dependent decay. Consequently, based on the results for *N*-methylphthalimide and **1** where the decay is pH dependent, the observed quenching rate constant may tentatively be assigned to the sum of rate constants for the reaction of protonation and decarboxylation of the radical anion, which are subsequent to fast equilibration of the triplet excited state and the triplet charge transfer species formed by PET (see Scheme 2).

Table 6. Properties of the triplet excited state obtained by LFP.

Comp.	τ (CH_3CN) / µs [a]	Φ_{ISC} [b]	$k_{q\,O2}$ / dm^3 mol^{-1} s^{-1} [c]	τ (pH 4) / µs [d]	τ (pH 7) / µs [e]
1	13 [f] 1.2	0.22 [f]	2×10^9 [f]	1.8 ± 0.4	0.34 ± 0.04 150 ± 50
2	0.62 ± 0.02	0.08 ± 0.02	(5.5 ± 0.7) × 10^8	0.90 ± 0.09	0.4 ± 0.3 6 ± 1 30-100
3	17 ± 1	0.15 ± 0.05	(3.1 ± 0.1) × 10^9	0.020 ± 0.002 12 ± 1 30-60	0.023 ± 0.006 6.0 ± 0.6 20-30
4	0.45 ± 0.05	0.15 ± 0.05	(3.6 ± 0.2) × 10^9	0.30 ± 0.05 6.5 ± 0.3	7 ± 1 20-100
5	< 0.01	-	-	-	-
6	0.29 ± 0.01 6.4 ± 0.4	-	(1.2 ± 0.1) ×10^{10}	-	-

[a] Lifetime of the triplet excited state in N_2-purged CH_3CN solution. The average value from at least three decays measured at three wavelengths is reported, and the errors correspond to the maximum absolute deviation. [b] Quantum yield of intersystem crossing in CH_3CN estimated by comparison of the intensity of the transient absorption immediately after the laser pulse of the optically matched solution at the excitation wavelength (266 nm) with the one of *N*-methylphthalimide (Φ_{ISC} = 0.8).[70] [c] Rate constant for the quenching of the triplet excited state by O_2 in CH_3CN. [d] Decay times for the transients detected in N_2-purged CH_3CN-H_2O (1:1 - v/v) in the presence of potassium phosphate buffer (c = 0.05 mol dm^{-3}) at pH = 3.8. [e] Decay times for the transients detected in N_2-purged CH_3CN-H_2O (1:1- v/v) in the presence of potassium phosphate buffer (c = 0.05 mol dm^{-3}) at pH = 7.0. [f] Taken from reference 44.

Compound **2** has two carboxylic functional groups. Therefore, it is plausible that efficient PET takes place only if the adamantane carboxylic acid is deprotonated, and the one at the phthalimide is not. Thus, at pH 7 it is likely that **2** exists in an equilibrium between mono- and dianionic species, that may have different triplet excited state lifetimes because the monoanionic species undergoes PET and the dianionic does not. Indeed, at pH 7, we detected three transients with the lifetimes of 0.4, 6 and 30-100 µs (Figure S31). Tentatively, the shorter lived two transients may be assigned to the triplet excited states (quenched or not), whereas the longest lifetime probably corresponds to the phthalimide radical anion or ketyl radical. From the two lifetimes at pH 4 and 7 (0.9 and 0.4 µs, respectively), the estimated quenching rate constant is $k_q \approx 1 \times 10^6$ s^{-1}, but the weakness of the transient signals precluded the precise determination of decay kinetics. Note the small value of the estimated rate constant, which cannot be attributed to PET, and which is in accord with the above discussion for **1**. However, the transient absorption spectra show different maxima depending on pH (Fig 6), in agreement with the detection of the triplet

excited state (at pH 4) and the phthalimide radical anion or the ketyl radical (at pH 7).

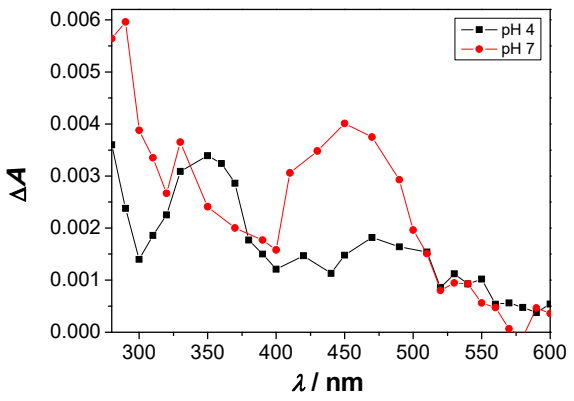

Figure 6. Transient absorption spectra for **2**, detected 200 ns after the laser pulse in N_2-purged CH_3CN-H_2O (1:1 - v/v) in the presence of phosphate buffer at pH 4 and 7.

It is plausible that compounds **3** and **4** undergo PET from S_1 and from the triplet excited state. Therefore, it is anticipated that the phthalimide radical anion and ketyl radicals can be formed by two rate constants, fast from S_1 and slower from the triplet state. However, comparison of the transient absorption spectra at two pH values for **3** is not very informative, although the transient assigned to the triplet excited state decays faster at pH 7. The estimated lifetimes of 12 or 6 µs correspond to $k_q = (8 \pm 2) \times 10^4$ s^{-1}, which is too slow for PET, similar to rates estimated for **1** and **2**. In addition, a very short-lived transient (≈ 20 ns) was detected at both pH values for **3**, whose assignment is beyond the scope of this manuscript. On the other hand, a pronounced difference between the spectra for **4** at two pH values was observed, where a new absorption band at ≈ 475 nm was detected at pH 7, tentatively attributed to the phthalimide radical anion or ketyl radicals. However, no significant difference in decay kinetics for the triplet excited state was observed, which may be due to inefficient decarboxylation photochemical reaction for triplet **4** (Table 2).

Photochemical reaction mechanisms

Preparative irradiations, fluorescence and LFP measurements provided a full description of photophysical and photochemical pathways for differently substituted phthalimides, whose understanding is important for the rational applications in synthesis. Results obtained from the experiments using acetone as a solvent will be discussed first. Upon irradiation in acetone, sensitization takes place and phthalimide triplet excited states are populated that react in intramolecular PET reactions with the deprotonated carboxylic group, leading efficiently to the decarboxylation products **1H**-**6H**. The exceptions are compounds **4**-**6**, where the substituents on the phthalimide significantly affected the photophysical properties and photochemical reactivity of the chromophore. Nitro group changed the pathways, making the molecule more like nitrobenzene derivative that has a very short triplet excited state lifetime due to the fast radiationless deactivation producing ground state molecules and the intrinsic reactivity of the nitro group. Therefore, in addition to **5H** which was formed inefficiently, some unidentified products resulting from nitrobenzene photochemistry were detected, whose isolation was impossible due to instability. The measured quantum yield for **5** reported in Table 2 corresponds to both processes, decarboxylation and those typical for the nitrobenzene chemistry. On the other hand, the strong electron-donating amino group in **6** decreased the energy of the triplet state so that PET from the carboxylate was not thermodynamically feasible. The OH group in **4** also has an electron-donating character, but the PET is still feasible. However, PET initiated processes were inefficient due to concomitant H-transfer reactions from the phenolic OH that quenches triplet excited states.

Lifetimes of triplet excited states at different pH values where PET was anticipated (or not) were analyzed providing apparent rate constants, which are too small to correspond to PET. Therefore, we propose that equilibration of the excited state with the CT species by PET and back electron transfer takes place, and the observed rate constant corresponds to the decay of the radical anion by sum of rate constants for protonation and decarboxylation. Such a mechanistic scenario is also in accord with the observed primary deuterium isotope effect on the photochemical conversion (see Scheme 3).

Upon direct excitation of **1**-**6** at 300 nm, the phthalimide S_1 states are populated, that contrary to *N*-alkylphthalimides do not undergo very efficient ISC. Properties of the excited states for **1** **3**, **4** and **6** are given in Table 7. Nevertheless, triplet excited state can be populated to some extent after direct excitation, which is followed by decarboxylation, but it is plausible that the reaction would be less efficient. Indeed, for **1**-**3** and **5** the Φ_R is lower in CH_3CN than in the presence of acetone. The same trend probably does not hold for **4**, that is prone to H-transfer reactions. This process significantly quenches triplets, and less likely singlet excited states. Moreover, the charge-transfer triplet state of **6** has too low energy and undergoes very inefficiently (or not at all) the PET with the carboxylate.

Phthalimides with electron-donating substituents **3**, **4** and **6** are fluorescent, and due to low Φ_{ISC} in aqueous solvent the photoreactions from S_1 compete with other deactivation pathways. Note that Φ_F for **3**, and somewhat for **6**, decreases in the pH region where the carboxylic group is deprotonated. Concomitantly, there is an increase in the photodecarboxylation efficiency for these two compounds, strongly indicating that the PET and decarboxylation dominantly take place from S_1. Shortening of the singlet excited state

Table 7. Photophysical properties of **1**, **3**, **4**, and **6**

View Article Online
DOI: 10.1039/D0NJ03465G

Comp.	E_{S1} / kJ mol^{-1} [a]	Φ_F (CH_3CN) [b]	τ_F (CH_3CN) /ns [c]	Φ_{ISC} (CH_3CN) [d]	τ_T (CH_3CN) /μs [e]
1	356	$< 10^{-4}$	n.d.	0.22	1.2
3	310	0.024 ± 0.002	1.68 ± 0.01 16.0 ± 0.4	0.15 ± 0.05	17 ± 1
4	308	0.037 ± 0.003	2.33 ± 0.8 14.7 ± 0.3	0.15 ± 0.05	0.45 ± 0.05
6	260	0.66 ± 0.03	17.2± 0.2	n.d.	0.29 ± 0.01 6.4 ± 0.4

[a] Energy of the singlet excited state. [b] Quantum yield of fluorescence in CH_3CN. [c] Lifetime of singlet excited state. [d] Quantum yield of intersystem crossing. [e] Lifetime of triplet excited state.

lifetimes allowed for the estimation of the rate constants for PET, which is for **3** two order of magnitudes larger. It is plausible that PET occurs also from the S_1 state of **4**, but the reaction may proceed efficiently only in the narrow pH region when the carboxylic functional group is deprotonated and the phenol is not. Formation of the phenolate probably significantly hampers the PET due to increase of the electron density on the phthalimide. LFP data allowed for the detection of triplet excited states of **3** and **4**, which can also undergo PET, as indicated from the irradiation experiments with acetone as sensitizer. The spin selectivity for the PET reaction in these compounds depends on the rate constants for fluorescence, PET and ISC. Apparently, electron donors on the phthalimide affect the photophysics in a way to make the ISC inefficient (probably by slowing down the nonradiative deactivation) and thus, facilitate the reactions from singlet excited states. Note that the photoreactions from S_1 still involve PET and back electron transfer because **3^{-}*** (S_1), **[3^{-}CT]*** and **3-AN** are not mesomeric structures since the system is not conjugated.

Photochemical reactions in CH_3CN gave in addition to simple decarboxylation products **1H**-**6H**, alcohols, peroxides, and ketones. Whereas alcohols and peroxides are formed by trapping the adamantyl radical by O_2, the mechanism for the formation of ketones needs further discussion. We postulated two pathways for the formation, that involve back electron transfer from the phthalimide radical anion to adamantyl radical giving anion, or radical pathways (Scheme 3). Taking the potential of the adamantyl radical reduction to anion (E_{red} = -2.19 V vs. Fc^0/Fc^+),[73,74] and the measured reduction potentials for phthalimides (Table 3), it is unlikely that back electron transfer takes place, except for those that have electron-donating substituent. Thus, the carbanion mechanism is plausible only for derivatives with electron donating substituents, such as OCH_3. Nevertheless, finding pathways that involve PET, subsequent chemical transformations and back electron transfer, which can initiate more chemical steps may have important impact in the design of new photocatalytic pathways, where phthalimide derivatives would be used as catalysts.

Conclusions

Photophysical properties and photochemical reactivity of adamantane carboxylic acid covalently attached to differently substituted phthalimides were investigated and put in connection with redox properties. Quantum yields of the reaction (Φ_R) greatly depend on pH, being much higher when the carboxylic acid is deprotonated, in line with the photoinduced electron transfer (PET) taking place from the carboxylate to the phthalimide in the excited state. Compounds bearing electron donor groups NH_2, OH and OCH_3 are fluorescent (Φ_F = 0.02-0.66). For the compounds substituted with OH and OCH_3, the PET takes place from both singlet and triplet excited states. The quantum yield of the triplet population by intersystem crossing (Φ_{ISC}) depends on the substituent at the phthalimide, and is much lower than for *N*-methylphthalimide. Therefore, the phthalimide substituents have a profound effect on the photophysics and spin selectivity in the photochemical reactions. LFP measurements in aqueous solutions at different pH values allowed for the detection of the triplet excited states, whose lifetimes depend on pH. Based on LFP and deuterium labeling experiments in preparative irradiation, a photochemical reaction mechanism was proposed that includes equilibration of the excited state (singlet or triplet) with the CT state by PET and back electron transfer, respectively. The shortening of the triplet lifetimes at pH 7 provided quenching constants which were assigned to the sum of rate constants corresponding to the decay of phthalimide radical anion by protonation and decarboxylation. Consequently, we have compelling evidences that after initial PET, back electron transfer is in competition with the subsequent reactions involving decarboxylation or protonation of the phthalimde radical anion, determining the overall efficiency of the decarboxylation process. A thorough understanding of different pathways in phthalimide photophysics and photochemistry presented herein highlights plausible processes that largely depend on the phthalimide substituents and the solution pH, understanding of which is important for the rational use of phthalimide derivatives in organic synthesis and photocatalytic processes.

Experimental

General

^{1}H and ^{13}C NMR spectroscopic data were recorded at room temperature on Bruker Avance 300 MHz or Bruker Avance 600 MHz spectrometer. $CDCl_3$, DMSO-d_6 or CD_3OD was used as deuterated solvent. TMS (^{1}H NMR) or deuterated solvent itself (^{13}C NMR) was used as internal reference. Chemical shifts were reported in ppm. ^{13}C NMR spectra were recorded in the APT technique or fully decoupled (denoted as COM in the ESI). IR spectra were recorded with a FT-IR ABB Bomem MB102 (samples as KBr pellets) or FT-IR ATR PerkinElmer UATR Two spectrometer (*neat* samples). The frequencies of the characteristic bands are reported in cm^{-1}. Melting points were measured on an Original Kofler Mikroheiztisch apparatus and were not corrected. HRMS data were obtained on Applied Biosystems DE STR MALDI-TOF/TOF instrument. Irradiation experiments were performed in a Rayonet RPR-100 photoreactor equipped with 10 lamps with the maximum output at ≈ 300 nm (1 lamp 8 W). During the irradiations, the irradiated solutions was placed in a quartz vessel (ϕ = 3.0 cm), that was placed in the center of the irradiated chamber, 7.5 cm separated from each lamp surrounding the vessel. The irradiated solutions were continuously purged with Ar and cooled by a tap water finger condenser. Solvents for the irradiations were of HPLC purity. Chemicals were purchased from the usual commercial sources and used as received. Solvents for chromatographic separations were used as is from the supplier (p.a. or HPLC grade) or purified by distillation (CH_2Cl_2).

Preparative photochemistry of substituted phthalimide derivatives - general procedure

A glass vessel (200 mL) was charged with the compound **2**-**6** (0.30 mmol) and K_2CO_3 (0.30 mmol, 1 equiv. for **2**, and 0.15 mmol, 0.5 equiv. for other compounds); dissolved in CH_3CN or acetone (150 mL) and H_2O (50 mL). The resulting solution was purged with Ar for 30 min and then irradiated in a reactor (10 lamps, 300 nm). H_2O (150 mL) was added, and an extraction with CH_2Cl_2 (5 × 100 mL) was carried out. The organic layers were dried over anhydrous $MgSO_4$ and filtered, and the solvent was removed on a rotary evaporator. Chromatography of the remaining residue on a silica gel column using Et_2O in CH_2Cl_2 (0 → 100%) or EtOAc in CH_2Cl_2 (0 → 100%) as eluent afforded pure photoproducts.

Preparative photochemistry of 2 and 3 in acetone as a sensitizer

Following the general procedure, irradiation of **2** followed by purification gave **2H** (81 mg, 81%) as colorless solid. Irradiation of **3**, followed by purification, gave **3H** (88 mg, 88%) as colorless solid. Characterization of **2**, **2H**, **3** and **3H** was reported.[57]

Preparative photochemistry of 3 without a sensitizer

Following the general procedure irradiation of **3** followed by purification gave **3H** (66 mg, 70%), **3COCH$_3$** (13 mg, 12%) and **3OH** (4 mg, 4%), all as colorless solids. Characterization of **3**, **3H** and **3OH** was reported.[57]

3-Acetyl-1-[*N*-(4'-methoxy)phthalimido]adamantane (**3COCH$_3$**) m.p. 102-104 °C; ^{1}H NMR (600 MHz, $CDCl_3$): δ = 7.66 (d, J = 8.2 Hz, 1H), 7.22 (d, J = 2.1 Hz, 1H), 7.13 (dd, J = 8.2, 2.1 Hz, 1H), 3.91 (s, 3H), 2.53-2.59 (m, 4H), 2.45 (d, J = 12.1 Hz, 2H), 2.32 (br s, 2H), 2.14 (s, 3H), 1.86 (d, J = 12.1 Hz, 2H), 1.76-1.82 (m, 3H), 1.66 ppm (d, J = 12.5 Hz, 1H); ^{13}C NMR (150 MHz, $CDCl_3$): δ = 212.5 (s), 169.7 (s), 169.6 (s), 164.7 (s), 134.5 (s), 124.5 (d), 124.0 (s), 120.2 (d), 107.1 (d), 60.3 (s), 56.2 (q), 48.7 (s), 40.5 (t), 39.5 (t, 2C), 37.2 (t, 2C), 35.4 (t), 29.5 (d, 2C), 24.7 ppm (q); IR (*neat*): ν = 2909, 2853, 1762, 1696, 1620, 1490, 1355, 1283, 1079, 745 cm^{-1}; HRMS (MALDI): m/z calcd for $C_{21}H_{23}NO_4$+H$^+$: 354.1705; found: 354.1706.

Preparative photochemistry of 4 without a sensitizer

Following the general procedure irradiation of **4** followed by purification gave **4H** (37 mg, 42%), **4COCH$_3$** (4 mg, 4%), **4OH** (15 mg, 16%) and **4OOH** (8 mg, 8%) as colorless solids, as well as recovered **4** (30 mg, 29% of starting amount).

3-Acetyl-1-[*N*-(4'-hydroxy)phthalimido]adamantane (**4COCH$_3$**) m.p. 128-131 °C; ^{1}H NMR (300 MHz, CD_3OD): δ = 7.55-7.61 (m, 1H), 7.03-7.11 (m, 2H), 2.53 (br s, 2H), 2.43-2.57 (m, 4H), 2.28 (br s, 2H), 2.15 (s, 3H), 1.76-1.90 (m, 5H), 1.71 ppm (d, J = 12.4 Hz, 1H); ^{13}C NMR (75 MHz, CD_3OD): δ = 215.0 (s), 171.1 (s), 170.9 (s), 164.8 (s), 135.8 (s), 125.6 (d), 123.6 (s), 121.6 (d), 110.0 (d), 61.1 (s), 49.9 (s), 41.5 (t), 40.5 (t, 2C), 38.3 (t, 2C), 36.3 (t), 30.9 (d, 2C), 24.7 ppm (q); IR (*neat*): ν = 3331, 2915, 2852, 1761, 1683, 1605, 1467, 1333, 1315, 1301, 1213, 1075, 978, 749, 637 cm^{-1}; HRMS (MALDI) m/z calcd for $C_{20}H_{21}NO_4$+H$^+$: 340.1549; found: 340.1541.

3-[*N*-(4'-Hydroxy)phthalimido]adamantane-1-hydroperoxide (**4OOH**) m.p. 218-220 °C; ^{1}H NMR (300 MHz, CD_3OD): δ = 7.53-7.61 (m, 1H), 7.02-7.10 (m, 2H), 2.56 (br s, 2H), 2.29-2.51 (m, 6H), 1.76 (d, J = 11.1 Hz, 2H), 1.66-1.80 (m, 3H), 1.60 ppm (d, J = 12.7 Hz, 1H); ^{13}C NMR (150 MHz, CD_3OD) δ = 171.0 (s), 170.8 (s), 164.8 (s), 135.8 (s), 125.6 (d), 123.6 (s), 121.6 (d), 110.0 (d), 81.0 (s), 62.6 (s), 43.9 (t), 40.4 (t, 2C), 40.0 (t, 2C), 36.3 (t), 32.0 ppm (d, 2C); IR (*neat*): ν = 3176, 2915, 2852, 1759, 1682, 1607, 1464, 1336, 1304, 1263, 1081, 978, 745, 639 cm^{-1}; MS (+ESI): m/z 330; MS (-ESI): m/z 328; HRMS (MALDI) m/z calcd for $C_{18}H_{19}NO_5$+Na$^+$: 352.1161; found: 352.1152.

Preparative photochemistry of 5 without a sensitizer

Following the general procedure for preparative photochemistry of substituted phthalimide derivatives, irradiation of **5**, followed by purification, gave **5H** (8 mg, 8%), **5OH** (15 mg, 15%) and **5OOH** (6 mg, 6%) as colorless solids, as well as recovered **5** (56 mg, 50% of starting amount). Characterization of **5**, **5H** and **5OH** was reported.[57]

3-[*N*-(4'-Nitro)phthalimido]adamantane-1-hydroperoxide (**5OOH**) m.p. 128-131 °C; ^{1}H NMR (300 MHz, $CDCl_3$): δ = 8.52-8.62 (m, 2H), 7.97 (d, J = 7.9 Hz, 1H), 7.61 (s, 1H), 2.64 (s, 2H), 2.34-2.54 (m, 6H), 1.94 (d, J = 11.7 Hz, 2H), 1.67-1.83 (m, 3H), 1.61 ppm (d, J = 12.7 Hz, 1H); ^{13}C NMR (75 MHz, $CDCl_3$): δ = 167.5 (s), 167.2 (s), 151.9 (s), 136.2 (s), 133.2 (s), 129.2 (d), 124.2 (d), 118.4 (d), 80.8 (s), 62.9 (s), 42.5 (t), 39.2 (t, 2C), 38.6 (t, 2C), 35.0 (t), 30.5 ppm (d, 2C); IR (KBr): ν = 3443, 2918, 2862, 1712, 1542, 1344, 1326, 1309, 1089, 720 cm^{-1}; HRMS (MALDI): m/z calcd for $C_{18}H_{18}N_2O_6$+H$^+$: 359.1243; found: 359.1243.

Irradiation of 3 in CH_3CN-D_2O

A glass vessel (200 mL) was charged with **3** (27.4 mg, 0.077 mmol), K_2CO_3 (5.40 mg, 0.039 mmol, 0.5 equiv.), dissolved in CH_3CN (37.5 mL) and H_2O (12.5 mL) or D_2O (12.5 mL). The resulting solution was purged with Ar for 30 min and then irradiated in a reactor (15 lamps, 300 nm) for 10 minutes. HPLC analysis of both solutions was carried out after the irradiation. Removal of the solvent by evaporation and chromatography of the remaining residue on a silica gel column by using Et_2O/CH_2Cl_2 (0 → 100%) as eluent gave **3H** and **3D**. The amount of deuterium in **3D** was determined by HPLC-MS analysis.

Photolyses of 2, 4 and 6 at different pH values

Quartz test tubes were charged with the solution (10 mL) of the phthalimide derivatives (c = 10^{-3} mol dm^{-3}) in CH_3CN-H_2O (1:1 - v/v) or acetone-H_2O (1:1 - v/v) in the presence of phosphate buffer (H_3PO_4-KH_2PO_4, KH_2PO_4-K_2HPO_4 or K_2HPO_4-K_3PO_4) with different pH values (total phosphate c = 0.05 mol dm^{-3}). The resulting solutions were purged with N_2 for 30 minutes and then irradiated in a reactor (8 lamps, 300 nm). The composition of the irradiated solution was analyzed by HPLC.

Photodecarboxylation quantum yields

Quartz test tubes were charged with the solution of phthalimide **1**-**6** (c = 10^{-3} mol dm^{-3}, 10 mL) in CH_3CN-H_2O (1:1 - v/v) or acetone-H_2O (1:1 - v/v) in the presence of phosphate buffer (KH_2PO_4-K_2HPO_4, total phosphate c = 0.05 mol dm^{-3}) at pH 4.5 or pH 8.3. Phthalimide **7** with the known photodecarboxylation quantum yield (Φ_R = 0.3)[42,60] was used as a secondary actinometer. To the solution of **7** (c = 10^{-3} mol dm^{-3}, 10 mL), K_2CO_3 (0.5 equiv.) was added. The resulting solutions were purged with N_2 for 30 min and then irradiated in a reactor (8 lamps, 300 nm in acetone or 254 nm in CH_3CN). The composition of the irradiated solutions was determined by HPLC. The photodecarboxylation quantum yields were calculated according to Eq S1.

UV-Vis and fluorescence measurements

UV-Vis and fluorescence measurements were conducted in CH_3CN or in CH_3CN-H_2O (1:1 - v/v) or (1:9 - v/v) in the presence of potassium phosphate buffer (c = 0.05 mol dm^{-3}) at pH 4.5 and 8.3. For the fluorescence measurements, the solutions were purged with Ar for 20 min. Emission spectra were recorded in the range 360-690 nm by exciting samples at three different wavelengths (330, 340 and 350 nm). The excitation slit was set to the bandpass of 2.5 or 5 nm, and the emission to 5 nm. Fluorescence quantum yields were determined using quinine sulfate in 0.5 mol dm^{-3} H_2SO_4 (Φ_F = 0.55) or 9-cyanoanthracene in cyclohexane (Φ_F = 0.92) as reference.[59] Quantum yields were calculated according to Eq S3. The measurements were conducted at 25 °C.

Time-resolved fluorescence measurements

Time-resolved fluorescence was measured with a time-correlated single-photon counting instrument described in literature previously.[75] The samples were excited with a pulsed diode laser at 368 nm. The pulse width was ~70 ps. The fluorescence signals were monitored at several wavelengths with a Hamamatsu R3809U-51 microchannel plate photomultiplier, which was connected to a Picoquant Timeharp 100 electronics having 36 ps/channel time resolution. For the instrument response function, silica in H_2O was used as scatterer. The decays were fit with a sum of exponentials according to Eq S4 using Picoquant FluoFit software.

UV-Vis pH titration for 4 and 4H

A set of quartz cells (2.5 mL) were charged with the solution of **4** (c = 2.72 × 10^{-5} mol dm^{-3}) or **4H** (c = 3.30 × 10^{-5} mol dm^{-3}) in CH_3CN-H_2O (1:9 - v/v) mixture in the presence of phosphate buffer (KH_2PO_4-K_2HPO_4, c = 0.05 mol dm^{-3}). Prior to the UV-Vis measurements, the pH of the solution was measured by a pH meter (Mettler, Toledo, Seven Multi). The measurements were conducted at 25 °C. The data were processed by multivariate nonlinear regression analysis by fitting to one-step protonation model with the Specfit software.

UV-Vis and fluorescence titration of 6 and 6H

A vial (10 mL) was charged with the solution of **6** (c = 1.75 × 10^{-5} mol dm^{-3}) or **6H** (c = 1.84 × 10^{-5} mol dm^{-3}) in CH_3CN-H_2O (1:9 - v/v) in the presence of KCl (c = 2 mol dm^{-3}). After measurement of the solution pH by a pH meter, a part of the solution was transferred to a quartz cell (2.5 mL), absorption and emission spectra were recorded, and then the solution was returned to the vial. To the solution aliquots of H_2SO_4 (c = 0.5 mol dm^{-3}) were added, and after each addition pH was measured, as well as absorption and emission spectra. For the fluorescence measurements, excitation slit was set to a bandpass of 5 nm and emission slit to 10 nm. The excitation was 370 nm, and the emission was collected in the range 380-730 nm. The measurement was conducted at 25 °C. The data was processed by multivariate nonlinear regression analysis by fitting to one-step protonation model with the Specfit software.

Fluorescence pH titration of 3 or 6

A set of quartz cells (2.5 mL) were charged with the solution of **3** (c = 9.13 × 10^{-6} mol dm^{-3}) or **6** (c = 1.76 × 10^{-5} mol dm^{-3}) in CH_3CN-H_2O (1:9 - v/v) in the presence of phosphate buffer (KH_2PO_4-K_2HPO_4, c = 0.05 mol dm^{-3}). Prior to the fluorescence measurements, the pH of the solution was measured by a pH meter. For the measurement of emission spectra, the excitation slit was set to a bandpass of 5 nm, and the emission slit to 10 nm, or both slits to 5 nm in case of **3**. The excitation for **3** was 350 nm, and the emission was collected in the range 360-610 nm. The excitation for **6** was 370 nm, and the emission was collected in the range 380-730 nm. The measurements were conducted at 25 °C. The data was processed by multivariate nonlinear regression analysis by fitting to one-step protonation model with the Specfit software.

Laser flash photolysis

The measurements were performed on a LP980 Edinburgh Instruments spectrometer. For the excitation the fourth harmonic of a Qsmart Q450 Quantel YAG laser was used. The pulse duration was 7 ns. For the measurement of spectra, the energy of the laser pulse at 266 nm was set to 20 mJ, and in some cases it was lower (8 mJ). Decay traces were measured with lower energy of the pulse (8 mJ) to avoid quenching by triplet-triplet annihilation. Absorbances of the solutions at the

excitation wavelength were set to 0.3. For the measurements of decay kinetics, static cells were used, which were frequently exchanged to assure no absorption of light by photoproducts. The spectra were measured in flow cells. The solutions were purged for 20 min with N_2 or O_2 prior to the measurements.

Cyclic voltammetry

Cyclic voltammetric measurements were carried out using the computer-controlled electrochemical system Autolab PGSTAT 30 (Eco-Chemie, Utrecht, Netherlands) equipped with GPES software. A three-electrode system (Methrom, Switzerland) with glassy carbon electrode (GCE) of 3 mm in diameter as a working electrode, Ag/AgCl (in 3 mol dm^{-3} NaCl) as a reference electrode and a platinum wire as a counter electrode were used. All potentials were expressed versus the Ag/AgCl (in 3 mol dm^{-3} NaCl) reference electrode. For the supporting electrolyte, 0.1 mol dm^{-3} NBu_4PF_6 in CH_3CN was used. The supporting electrolyte was placed in the electrochemical cell and the required aliquot of the standard analyte solution was added. The solution in the electrochemical cell was deaerated with high purity nitrogen for 10 min before measurement, and the nitrogen blanket was maintained thereafter. Before each run, the glassy carbon (GC) working electrode was polished with diamond suspension in spray (grain size 6 µm) and rinsed with ethanol and deionised water. Cyclic voltammetry on GC electrode was performed for all compounds using a potential step increment of 2 mV and a scan rate of 500 mV s^{-1} (except for **2** where scan rate was 100 mV s^{-1}). All experiments were performed at room temperature and each individual measurement was repeated three times.

Conflicts of interest

There are no conflicts to declare.

Acknowledgements

These materials are based on work financed by the Croatian Science Foundation (HRZZ IP-2014-09-6312 for NB). The authors thank Dr. Blaženka Gašparović for the support and help in conducting cyclic voltammograms. LB acknowledges the support of the National Research, Development and Innovation Office of Hungary (Grant K123995 and BIONANO GINOP-2.3.2-15-2016-00017).

Notes and references

1 Y. Kanaoka, *Acc. Chem. Res*., 1978, **11**, 407-413.
2 M. Horvat, K. Mlinarić-Majerski, N. Basarić, *Croat. Chem. Acta*, 2010, **83**, 179-188.
3 A. G. Griesbeck, N. Hoffmann, K.-D. Warzecha, *Acc. Chem. Res*., 2007, **40**, 128-140.
4 M. Oelgemöller, A. G. Griesbeck, in *CRC Handbook of Organic Photochemistry and Photobiology*, 2nd Ed. (Eds.: W. Horspool, F. Lenci), CRC Press, Boca Raton, **2004**.
5 M. Oelgemöller, A. G. Griesbeck, *J. Photochem. Photobiol. C: Photochem. Rev*., 2002, **3**, 109-127.
6 U. C. Yoon, P. S. Mariano, in *CRC Handbook of Organic Photochemistry and Photobiology*, 2nd Ed. (Eds.: W. Horspool, F. Lenci), CRC Press, Boca Raton, **2004**.
7 U. C. Yoon, P. S. Mariano, *Acc. Chem. Res*., 2001, **34**, 523-533.
8 A. G. Griesbeck, A. Henz, K. Peters, E.-M. Peters, H. G. von Schnering, *Angew. Chem. Int. Ed.*, 1995, **34**, 474-476.
9 A. G. Griesbeck, T. Heinrich, M. Oelgemöller, J. Lex, A. Molis, *J. Am. Chem. Soc*., 2002, **124**, 10972-10973.
10 U. C. Yoon, Y. H. Jin, S. W. Oh, C. H. Park, J. H.; Park, C. F. Campana, X. Cai, E. N. Duesler, P. S. Mariano, *J. Am. Chem. Soc*., 2003, **125**, 10664-10671.
11 A. Soldevilla, A. G. Griesbeck, *J. Am. Chem. Soc*., 2006, **128**, 16472-16473.
12 A. G. Griesbeck, W. Kramer, J. Lex, *Angew. Chem. Int. Ed.*, 2001, **40**, 577-579.
13 Y.-J. Lee, D.-H. Ahn, K.-S. Lee, A. R. Kim, D. J. Yoo, M. Oelgemöller, *Tetrahedron Lett*., 2011, **52**, 5029-5031.
14 F. Hatoum, S. Gallagher, M. Oelgemöller, *Tetrahedron Lett*., 2009, **50**, 6593-6596.
15 F. Hatoum, J. Engler, C. Zelmer, J. Wißen, C. A. Motti, J. Lex, M. Oelgemöller, *Tetrahedron Lett*., 2012, **53**, 5573-5577.
16 A. G. Griesbeck, M. Oelgemöller, *Synlett*, **1999**, 492-494.
17 F. Hatoum, S. Gallagher, L. Baragwanath, J. Lex, M. Oelgemöller, *Tetrahedron Lett*., 2009, **50**, 6335-6338.
18 V. Belluau, P. Noeureuil, E. Ratzke, A. Skvortsov, S. Gallagher, C. A. Motti, M. Oelgemöller, *Tetrahedron Lett*., 2010, **51**, 4738-4741.
19 S. Gallagher, F. Hatoum, N. Zientek, M. Oelgemöller, *Tetrahedron Lett.*, 2010, **51**, 3639-3641.
20 F. Boscá, M. A. Miranda, *J. Photochem. Photobiol. B: Biol.*, 1998, **43**, 1-26.
21 F. Boscá, M.-L. Marín, M. A. Miranda, *Photochem. Photobiol.*, 2001, **74**, 637-655.
22 F. Boscá, M.-L. Marín, M. A. Miranda, in *CRC Handbook of Organic Photochemistry and Photobiology*, 2nd Ed. (Eds.: W. Horspool, F. Lenci), CRC Press, Boca Raton, **2004**.
23 S. Monti, S. Sortino, G. De Guidi, G. Marconi, *J. Chem. Soc., Faraday Trans*., 1997, **93**, 2269-2275.
24 L. J. Martínez, J. C. Scaiano, *J. Am. Chem. Soc*., 1997, **119**, 11066-11070.
25 G. Cosa, L. J. Martínez, J. C. Scaiano, *Phys. Chem. Chem. Phys.*, 1999, **1**, 3533-3537.
26 M. Laferrière, C. N. Sanram, J. C. Scaiano, *Org. Lett*., 2004, **6**, 873-875.
27 J. A. Blake, E. Gagnon, M. Lukeman, J. C. Scaiano, *Org. Lett*., 2006, **8**, 1057-1060.
28 Y. P. Chuang, J. Xue, Y. Du, M. Li, H.-Y. An, D. L. Phillips, *J. Phys. Chem. B*, 2009, **113**, 10530-10539.
29 M.-D. Li, Y. Du, Y. P. Chuang, J. Xue, D. L. Phillips, *Phys. Chem. Chem. Phys.*, 2010, **12**, 4800-4808.
30 Y. Xu, X. Chen, W.-H. Fang, D. L. Phillips, *Org. Lett*., 2011, **13**, 5472-5475.
31 M.-D. Li, C. S. Yeung, X. Guan, J. Ma, W. Li, C. Ma, D. L. Phillips, *Chem. Eur. J*., 2011, **17**, 10935-10950.
32 M.-D. Li, T. Su, J. Ma, M. Liu, H. Liu, X. Li, D. L. Phillips, *Chem. Eur. J*., 2013, **19**, 11241-11250.
33 F. Boscá, M. A. Miranda, G. Carganico, D. Mauleón, *Photochem. Photobiol.*, 1994, **60**, 96-101.
34 H. Huang, C. Yu, Y. Zhang, Y. Zhang, P. S. Mariano, W. Wang, *J. Am. Chem. Soc*. 2017, **139**, 9799-9802.
35 J. A. Kautzky, T. Wang, R. W. Evans, D. W. C. MacMillan, *J. Am. Chem. Soc*. 2018, **140**, 6522-6526.
36 N. A. Till, R. T. Smith, D. W. C. MacMillan, *J. Am. Chem. Soc*. 2018, **140**, 5701-5705.
37 T. Yamamoto, T. Iwasaki, T. Morita, Y. Yoshimi, *J. Org. Chem*. 2018, **83**, 3702-3709.
38 Q.-Q. Ge, J.-S. Qian, J. Xuan, *J. Org. Chem*. 2019, **84**, 8691-8701.

39 S. Senaweera, K. C. Cartwright, J. A. Tunge, *J. Org. Chem*. 2019, **84**, 12553-12561.
40 K. C. Cartwright, S. B. Lang, J. A. Tunge, *J. Org. Chem*. 2019, **84**, 2933-2940.
41 X. Zhang, P. Zhu, R. Zhang, X. Li, T. Yao, *J. Org. Chem*. 2020, **85**, 9503-9513.
42 L. Mandić, K. Mlinarić-Majerski, A. G. Griesbeck, N. Basarić, *Eur. J. Org. Chem*., **2016**, 4404-4414.
43 M. Sohora, T. Šumanovac Ramljak, K. Mlinarić-Majerski, N. Basarić, *Croat. Chem. Acta*, 2014, **87**, 431-446.
44 M. Horvat, K. Mlinarić-Majerski, A. G. Griesbeck, N. Basarić, *Photochem. Photobiol. Sci*., 2011, **10**, 610-617.
45 T. Šumanovac Ramljak, M. Sohora, I. Antol, D. Kontrec, N. Basarić, K. Mlinarić-Majerski, *Tetrahedron Lett*., 2014, **55**, 4078-4081.
46 M. Sohora, M. Vazdar, I. Sović, K. Mlinarić-Majerski, N. Basarić, *J. Org. Chem*., 2018, **83**, 14905-14922.
47 A. G. Griesbeck, S. Schieffer, *Photochem. Photobiol. Sci*., 2003, **2**, 113-117.
48 V. Wintgens, P. Valat, J. Kossanyi, A. Demeter, L. Biczók, T. Bérces, *New J. Chem*., 1996, **20**, 1149-1158.
49 M. Atar, B. Öngel, H. Riedasch, T. Lippold, J. Neudörfl, D. Sampedro, A. G. Griesbeck, *ChemPhotoChem*, 2020, **4**, 89-97**.**
50 T. Soujanya, R. W. Fessenden, A. Samanta, *J. Phys. Chem*., 1996, **100**, 3507-3512.
51 G. Saroja, T. Soujanya, B. Ramachandram, A. Samanta, *J. Fluoresc*., 1998, **8**, 405-410.
52 A. Morimoito, T. Yatsuhashi, T. Shimada, L. Biczók, D. A. Tryk, H. Inoue, *J. Phys. Chem. A*, 2001, **105**, 10488-10496.
53 D. E. Wetzler, C. Chesta, R. Fernández-Prini, P. F. Aramendía, *J. Phys. Chem. A*, 2002, **106**, 2390-2400.
54 V. Wintgens, C. Amiel, *J. Photochem. Photobiol. A: Chem*., 2004, **168**, 217-226.
55 D. C. Khara, S. Banerjee, A. Samanta, *ChemPhysChem*, 2014, **15**, 1793-1798.
56 P. Benčić, L. Mandić, I. Džeba, I. Tartaro Bujak, L. Biczók, B. Mihaljević, K. Mlinarić-Majerski, I. Weber, M. Kralj, N. Basarić, *Sens. Actuators: B: Chem*., 2019, **286**, 52-61.
57 L. Mandić, P. Benčić, K. Mlinarić-Majerski, S. Liekens, R. Snoeck, G. Andrei, M. Kralj, N. Basarić, *Arch Pharm*., 2020, **e2000024**. https://doi.org/10.1002/ardp.202000024.
58 R. J. Perkins, H.-C. Xu, J. M. Campbell, K. D. Moeller, *Beilstein J. Org. Chem*., 2013, **9**, 1630-1636.
59 M. Montalti, A. Credi, L. Prodi, M. T. Gandolfiln *Handbook of Photochemistry*; CRC Taylor and Francis: Boca Raton, **2006**.
60 H. Görner, M. Oelgemöller, A. G. Griesbeck, *J. Phys. Chem A*, 2002, **106**, 1458-1464.
61 A. Reiffers, C. Torres Ziegenbein, L. Schubert, J. Diekmann, K. A. Thom, R. Kühnemuth, A. G. Griesbeck, O. Weingart, P. Gilch, *Phys. Chem. Chem. Phys*., 2019, **21**, 4839-4853.
62 V. Wintgens, P. Valat, J. Kossanyi, L. Biczók, A. Demeter, T. Bérces, *J. Chem. Soc., Faraday Trans*., 1994, **90**, 411-421.
63 S. E. Braslawsky, *Pure Appl. Chem*., 2007, **79**, 293-465.
64 M. Albrecht, C. Bohne, A. Graznhan, H. Ihmels, T. C. S. Pace, A. Schnurpfeil, M. Waidelich, C. Yihwa, *J. Phys. Chem. A*, 2007, **111**, 1036-1044.
65 Z. Miskolczy, J. G. Harangozó, L. Biczók, V. Wintgens, C. Lorthioir, C. Amiel, *Photochem. Photobiol. Sci.,* 2014, **13**, 499-508.
66 D. W. Ellis, L. B. Rogers, *Spectrochim. Acta*, 1964, **20**, 1709-1720.
67 J. F. Ireland, P. A. H. Wyatt, *Adv. Phys. Org. Chem.*, 1976, **12**, 131-221.
68 L. G. Arnaut, S. J. Formosinho, *J. Photochem. Photobiol. A: Chem*., 1993, **75**, 1-20.
69 M. Horvat, H. Görner, K.-D. Warzecha, J. Neudörfl, A. G. Griesbeck, K. Mlinarić-Majerski, N. Basarić, *J. Org. Chem*., 2009, **74**, 8219-8231.
70 A. G. Griesbeck, H. Görner, *J. Photochem. Photobiol. A: Chem*., 1999, **129**, 111-119.
71 W. J. Leigh, E. C. Lathioor, M. J. St. Pierre, *J. Am. Chem. Soc*., 1996, **118**, 12339-12348.
72 S. Aich, C. Raha, S. Basu, *J. Chem. Soc., Faraday Trans*., 1997, **93**, 2991-2996.
73 D. Occhialini, J. S. Kristensen, K. Daasbjerg, H. Lund, *Acta Chem. Scand.*, 1992, **46**, 474-481.
74 T. Kjærsbo, K. Daasbjerg, S. U. Pedersen, *Electrochim. Acta*, 2003, **48**,1807-1816.
75 M. Megyesi, L. Biczók, *J. Phys. Chem. B* 2010, **114**, 2814-2819.

View Article Online
DOI: 10.1039/D0NJ03465G

ARTICLE Journal Name

View Article Online
DOI: 10.1039/D0NJ03465G

TOC Entry

View Article Online
DOI: 10.1039/D0NJ03465G

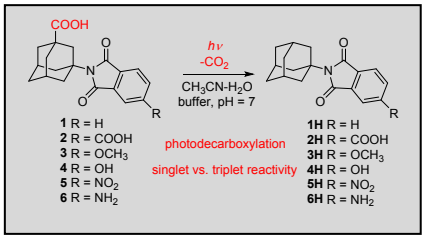

Substituents on the phthalimide affect its photophysics and photochemical reactivity. Electron donors generally result in low quantum yields of intersystem crossing and reactivity from singlet excited states.